CHEMISTRY
A EUROPEAN JOURNAL

DOI: 10.1002/chem.200601385

Osmium-Mediated C–H and C–C Bond Cleavage of a Phenolic Substrate: *p*-Quinone Methide and Methylene Arenium Pincer Complexes

Régis M. Gauvin,[a, b] Haim Rozenberg,[c] Linda J. W. Shimon,[c] Yehoshoa Ben-David,[a] and David Milstein*[a]

Abstract: The diphosphine 2,4,6-$(CH_3)_3$-3,5-$(i Pr_2PCH_2)_2C_6OH$ (**1**) reacts with $[OsCl_2(PPh_3)_3]$ in presence of an excess of triethylamine to yield the isomeric *para*-quinone methide derivatives $[Os\{4\text{-}(CH_2)\text{-}1\text{-}(O)\text{-}2,6\text{-}(CH_3)_2\text{-}3,5\text{-}(i Pr_2PCH_2)_2C_6\}(Cl)(H)(PPh_3)]$ (**2** and **3**), which differ in the positions of the mutually *trans* hydride and chloride ligands. Complex **2** reacts with CO to afford the dicarbonyl species $[Os\{1\text{-}(O)\text{-}2,4,6\text{-}(CH_3)_3\text{-}3,5\text{-}(i Pr_2PCH_2)_2C_6\}(Cl)(CO)_2]$ (**4**), which results from hydride insertion into the quinonic double bond. Protonation of **2** and **3** leads to the formation of the methylene arenium derivative $[Os\{4\text{-}(CH_2)\text{-}1\text{-}(OH)\text{-}2,6\text{-}(CH_3)_2\text{-}3,5\text{-}(i Pr_2PCH_2)_2C_6\}(Cl)(H)(PPh_3)]\text{-}[OSO_2CF_3]$ (**5a**). The diphosphine **1** reacts with $[OsCl_2(PPh_3)_3]$ at 100 °C under H_2 to afford $[Os\{1\text{-}(OH)\text{-}2,6\text{-}(CH_3)_2\text{-}3,5\text{-}(i Pr_2PCH_2)_2C_6\}(Cl)(H_2)(PPh_3)]$ (**6**), a PCP pincer complex resulting formally from $C(sp^2)$–$C(sp^3)$ cleavage of the $C\text{–}CH_3$ group in **1**. C–C hydrogenolysis resulting in the same complex is achieved by heating **2** under H_2 pressure. Reaction of the diphosphine substrate with $[OsCl_2(PPh_3)_3]$ under H_2 at lower temperature allows the observation of a methylene arenium derivative resulting from C–H activation, $[Os\{4\text{-}(CH_2)\text{-}1\text{-}(OH)\text{-}2,6\text{-}(CH_3)_2\text{-}3,5\text{-}(i Pr_2PCH_2)_2C_6\}(Cl)_2(H)]$ (**7**). This compound reacts with PPh_3 in toluene to afford the ionic derivative $[Os\{4\text{-}(CH_2)\text{-}1\text{-}(OH)\text{-}2,6\text{-}(CH_3)_2\text{-}3,5\text{-}(i Pr_2PCH_2)_2C_6\}(Cl)(H)(PPh_3)]Cl$ (**5b**). X-ray diffraction studies have been carried out on compounds **2**, **3**, **4**, **5b**, **6**, and **7**, which allows the study of the structural variations when going from methylene arenium to quinone methide derivatives.

Keywords: C–C activation · C–H activation · osmium · P ligands · quinone methides

Introduction

Quinone methides are an important class of compounds with relevance to several fields. For example, they play a central role in biologically relevant processes such as DNA cross-linking[1] or antitumoral activity,[2] and are also widely used as synthons in organic synthesis.[3] The *o*- and *p*-quinone methides can be thought of as formally neutral benzylic carbocations stabilized by electron donation from the oxygen anion substituent to the cationic benzylic carbon: this explains their high reactivity towards nucleophiles, and the elusiveness of simple quinone methides to isolation.[4]

Within the framework of our work on the activation of strong bonds,[5] we became interested in the field of metal-stabilized quinonoid compounds,[6] thus achieving, among others, coordination of a *p*-quinone methide fragment, either as "free" ligand onto Pd^0[7] or as a part of a chelating diphosphinic moiety onto Rh^I.[8] The latter approach also allowed the isolation of methylene arenium derivatives, upon reaction with strong electrophiles.[8b,9] Examples of *o*-quinone methides complexed onto Ir^I[10] and Os^{II}[11] and of their reactivity have been described.

In our studies on osmium-mediated C–C and C–H bond activation of nonstrained, diphosphinic substrates, we have shown that the osmium precursor $[OsCl_2(PPh_3)_3]$ reacts under hydrogen pressure with 2,4,6-$(CH_3)_3$-3,5-$(i Pr_2PCH_2)_2C_6H$ to afford a PCP pincer complex by C–C bond cleavage.[12] We then became interested in the comparative study of the reactivity of the phenolic derivative 2,4,6-$(CH_3)_3$-3,5-$(i Pr_2PCH_2)_2C_6OH$ (**1**). While this substrate is amenable to C–C bond activation, it also constitutes a suita-

[a] Dr. R. M. Gauvin, Y. Ben-David, Prof. Dr. D. Milstein
Department of Organic Chemistry, The Weizmann Institute
Rehovot, 76100 (Israel)
Fax: (+972) 893-44-142
E-mail: david.milstein@weizmann.ac.il

[b] Dr. R. M. Gauvin
Unité de Catalyse et de Chimie du Solide UMR CNRS
8181 ENSCL - BP 90108 59652 Villeneuve d'Ascq Cedex (France)

[c] Dr. H. Rozenberg, Dr. L. J. W. Shimon
Unit of Chemical Research Support, The Weizmann Institute
Rehovot, 76100 (Israel)

ble precursor for the formation of quinone methide derivatives upon coordination and C–H bond activation. We present here our results on quinone methide and methylene arenium osmium derivatives obtained from reaction of **1** with $[OsCl_2(PPh_3)_3]$, as well as on osmium-mediated C–C bond activation.

Results

Formation of quinone methide complexes: Room temperature reaction of the Os^{II} precursor $[OsCl_2(PPh_3)_3]$ with the diphosphine **1** in benzene in presence of an excess of triethylamine affords the bright orange isomeric quinone methide complexes $[Os\{4\text{-}(CH_2)\text{-}1\text{-}(O)\text{-}2,6\text{-}(CH_3)_2\text{-}3,5\text{-}(i\text{Pr}_2\text{PCH}_2)_2C_6\}(Cl)(H)(PPh_3)]$ **2** and **3** in a 2:1 ratio (Scheme 1). Following the reaction course by NMR spectroscopy indicated that the ratio between the regioisomers remains constant.

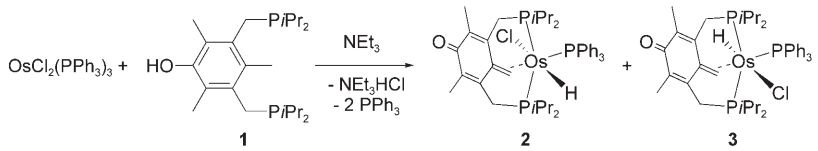

Scheme 1. Formation of quinone methides **2** and **3**.

The two isomers can be separated by fractional crystallization and their solid-state structures were determined by X-ray diffraction studies (Figures 1 and 2). These are the

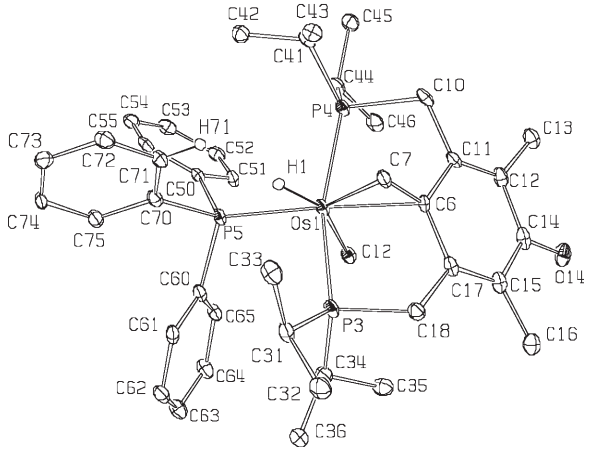

Figure 1. ORTEP view of **2** with the thermal ellipsoids at 30% of probability.

first examples of structurally characterized osmium-complexed *p*-quinone methides. For the sake of clarity of the discussions regarding the solid-state structures, the cyclic system carbon atoms are labeled as shown here.

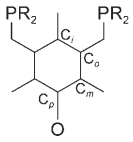

Both compounds adopt a distorted octahedral geometry, with the bis-chelating quinone methide diphosphine ligand bound through the two phosphorus atoms and the exocyclic double bond in a meridional arrangement. The triphenylphosphine ligand is located *trans* to the quinone methide double bound, while the chloride and hydride are located in the remaining two *cis* positions. The difference between the two isomers **2** and **3** lies in the arrangement of the mutually *trans* H and Cl ligands; in isomer **2**, the hydride is *cis* to the $=CH_2$, while in **3** this position is occupied by the chloride.

In the solid-state structure of **2**, the quinone methide structural type is confirmed by the expected features (selected bond lengths and angles are given in Table 1): the short C14–O14 distance of 1.254(7) Å is within the range of the C=O bond lengths, and the intracyclic C–C distances are characteristic of a 1,4-unsaturated ring, as shown by the alternation of long, short and long C–C bonds: the average C_i–C_o (C6–C11 and C6–C17), C_o–C_m (C11–C12 and C15–C17) and C_m–C_p (C12–C14 and C14–C15) bond lengths are 1.472(6),

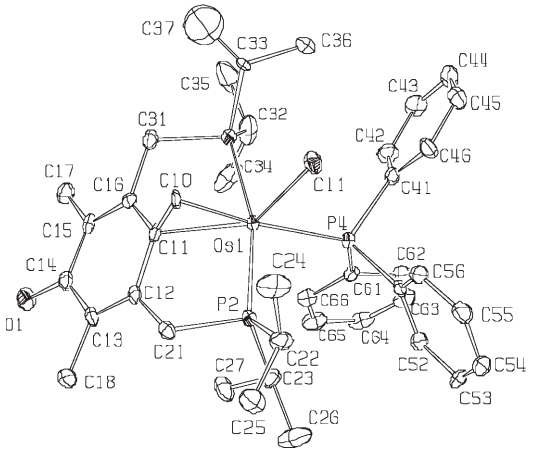

Figure 2. ORTEP view of one of the two independent molecules of **3** with the thermal ellipsoids at 30% of probability.

1.344(7), and 1.466(7) Å, respectively. The C6–C7 bond length of 1.453(7) Å is in the expected range for coordinated double bonds. The hydride was located, the Os–H bond length being within the expected range (Os1–H1 = 1.688(57) Å). It is relevant to note the short distance of 1.880 Å between H1 and H71, an *ortho*-proton of the coordinated triphenylphosphine. The corresponding phenyl ring is almost in the Os-P5-C70 plane (dihedral angle of 22.2°), probably in order to optimize a weak H–H interaction.

Table 1. Selected bond lengths [Å] and angles [°] of complex **2**.

Os1–C7	2.117(5)	C6–C11	1.480(6)
Os1–C6	2.255 (5)	C11–C12	1.348(8)
C6–C7	1.453(7)	C12–C14	1.460(8)
C14–O14	1.254(7)	C14–C15	1.472(7)
Os1–P3	2.400(2)	C15–C17	1.340(7)
Os1–P4	2.374(1)	C6–C17	1.464(7)
Os1–H1	1.688(57)	Os1–P5	2.391(2)
Os1–Cl2	2.471(1)		
P3-Os1-P4	162.77(4)	P5-Os1-H1	74.03(19)
Os1-C7-C6	75.8(3)	P5-Os1-Cl2	86.95(5)
C7-Os1-H1	70.60(15)		

In the solid-state structure of **3**, the quinone methide structural type is evidenced by the short C14–O1 distance of 1.245(9) Å, as well as by the expected bond length alternation within the ring (selected bond lengths and angles are given in Table 2): the average C_i–C_o (C11–C12 and C11–C16), C_o–C_m (C12–C13 and C15–C16) and C_m–C_p (C13–C14 and C14–C15) bond lengths are 1.473(11), 1.354(11), and 1.462(11) Å, respectively. The exocyclic double bond interaction with the metallic center is affected by the proximity of the bulky halide: this is noticeable through the longer Os1–C10 bond length of 2.155(7) Å compared to 2.117(5) Å in **2**. However, the shorter Os1–C11 distance (2.237(7) Å in **3** and 2.255(5) Å in **2**) and the comparable C10–C11 distance within the double bond (1.457(10) Å in **3** and 1.453(7) Å in **2**) seems to indicate that the bonding between the double bond and the metal in the two isomers is comparable. Although the hydride could not be located, it seems that an interaction between the hydride and an *ortho*-proton of the coordinated triphenylphosphine is present, as in **2**: the related phenyl ring is almost in the Os1-P4-C61 plane, as shown by the Os1-P4-C61-C6 dihedral angles of 10.9°.

Table 2. Selected bond lengths [Å] and angles [°] of complex **3**.

Os1–C10	2.155(7)	C14–O1	1.245(9)
Os1–C11	2.237(7)	C11–C12	1.476(11)
C10–C11	1.457(10)	C11–C16	1.470(10)
Os1–P2	2.356(2)	C12–C13	1.349(11)
Os1–P3	2.365(2)	C13–C14	1.456(10)
Os1–P4	2.419(2)	C14–C15	1.467(11)
Os1–Cl1	2.514(2)	C15–C16	1.360(10)
P2-Os1-P3	163.82(7)	C11-Os1-P4	155.30(19)
Os1-C10-C11	73.7(4)	P4-Os1-Cl1	81.50(7)
C10-Os1-P4	165.6(2)		

The structural features of the quinone methide moiety within **2** and **3** are similar to those of the structurally characterized Rh^I complexes **QM1** and **QM2**.[8] In these compounds, the average C_o–C_m bond has a clear double-bond character (1.351(8) Å in **QM1** and 1.359(12) Å in **QM2**), while the C_i-C_o (1.448(8) Å in **QM1** and 1.488(11) Å in **QM2**) and C_m-C_p (1.470(8) Å in **QM1** and 1.482(12) Å in **QM2**) bond lengths are closer to single bond type. The η^2-exocyclic double bond is significantly shorter in **QM1** and **QM2** (1.441(8) and 1.402(11) Å, respectively) than in **2** and **3** (1.453(7) and 1.457(10) Å, respectively), which may indicate a stronger interaction in the case of the osmium complexes. The C=O bond is also slightly longer in **2** (1.254(7) Å) and **3** (1.245(9) Å), than in **QM1** (1.239(6) Å) and **QM2** (1.241(10) Å).

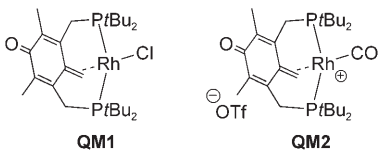

QM1 QM2

Solution NMR data for **2** is consistent with the solid-state structure. The $^{31}P\{^1H\}$ spectrum consists of a triplet (1P) and a doublet (2P), respectively centered at $\delta = -5.58$ and -7.83 ppm, with $^2J(P,P) = 16.1$ Hz. In the ^1H NMR spectrum, the $=CH_2$ protons resonate at $\delta = 3.76$ ppm as a doublet of triplets due to coupling with the two different phosphorus nuclei. For comparison, these protons resonate as multiplets centered at $\delta = 3.13$ and 5.23 ppm in **QM1** and **QM2**, respectively. The phosphinomethylene groups give rise to two sets of doublets of virtual triplets at $\delta = 2.87$ and 2.41 ppm. The OsH gives rise to a doublet of triplets signal centered at $\delta = -12.95$ ppm. $^{13}C\{^1H\}$ NMR also indicates that the quinonic structure observed in the crystalline state is retained in solution, as shown by the characteristic *C*=O singlet at $\delta = 185.77$ ppm, a value similar to those observed in **QM1** and **QM2**, that is, $\delta = 186.51$ and 184.93 ppm, respectively. The exocyclic double bond fragment signals consist of a doublet of triplets at $\delta = 68.38$ ppm for the quaternary carbon atom and a broad singlet at $\delta = 29.16$ ppm for the methylenic carbon atom. The analogous carbons resonate at $\delta = 66.97$ and 41.91 ppm in **QM1**, while the corresponding signals appear at $\delta = 100.36$ and 76.44 ppm, respectively, in the less electron-rich **QM2**. The assignments have been confirmed by DEPT and C–H correlation 2D NMR spectroscopy. The isomeric compound **3** displays spectroscopic features close to those of **2**: its $^{31}P\{^1H\}$ spectrum consists of a doublet at $\delta = -4.61$ ppm and a triplet at $\delta = -8.59$ ppm, with a coupling constant of 15.0 Hz. The coordinated double bond methylene protons appear in the ^1H NMR spectrum as a doublet of triplets centered at $\delta = 3.49$ ppm, while the hydride resonates at $\delta = -13.60$ ppm as a doublet of triplets. The ^{13}C NMR spectrum exhibit a singlet at $\delta = 184.87$ ppm for the carbonyl group, and two signals at $\delta = 38.78$ and 65.69 ppm for the methylene and quaternary carbon atoms of the exocyclic double bond, respectively. The infrared spectra of **2** and **3** exhibit the characteristic strong $\nu_{(C=O)}$ absorption band at 1629 and 1615 cm^{-1}, respectively.

A spin saturation transfer experiment carried out on a mixture of **2** and **3** at room temperature in deuterated chloroform does not exhibit exchange between the two isomers on the NMR timescale. This NMR experiment confirmed the assignment of the signals and structures of both **2** and **3**: irradiation of the hydride signal in both isomers revealed the proximity of the OsH and the *ortho*-PPh_3 protons, and between the OsH and the quinone methide meth-

ylenic protons only in the case of **2**, in which case an NOE signal was observed (Scheme 2)

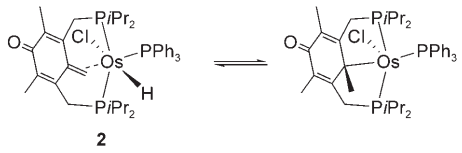

2

Scheme 2. Postulated dynamic processes in **2** (hydride insertion and β-H elimination).

Solutions of pure **2** or **3** are stable at room temperature for days in deuterated benzene or chloroform. However, in the presence of a weak acid such as NH_4Cl at room temperature, isomerization is observed. The mechanism of this process has not been clarified. Higher temperatures increase the isomerization rate. It is worth noting that these species are stable in ethanol, as already observed for η^2-Pd coordinated quinone methide,[7] which is an indication of the metal influence on the taming of the quinone methide fragment reactivity. The nucleophilic attack on the methylenic carbon atom does not proceed, contrary to what is observed for free quinone methides.

Exposure of a solution of **2** in $CDCl_3$ to excess D_2O leads to H-D exchange involving the hydride, quinone methide methylene protons and one of the diastereotopic phosphino methylenic positions (75, 45, and 30%, respectively) after 14 h. ^2H NMR measurements of the resulting species in $CHCl_3$ confirmed these observations and indicated some incorporation in the osmium-bound PPh_3 *ortho*-position. The observed H-D exchanges proceed most probably through OsH–D_2O exchange, followed by various intramolecular exchange processes. Reversible insertion of the coordinated double-bond into the Os–H bond[13] accounts for deuterium incorporation into the QM methylenic position, thus generating a transient σ-bound cyclohexadienonyl intermediate (Scheme 2). The phosphinomethylenic protons in pincer complexes are known to undergo exchange processes with hydride moieties,[14] presumably through deprotonation to generate the ylide form.[15] The observed stereospecificity of this D-incorporation tends to indicate the implication of an intramolecular pathway. Exchange of the *ortho*-PPh_3 protons relates to the well-documented *ortho*-metalation reaction.[16]

As mentioned, the reversible hydride insertion into the quinone methide double bond would generate a coordinatively unsaturated intermediate, which may be trapped by a donor ligand. Indeed, reaction of **2** with CO under moderate heating affords quantitatively [Os{1-(O)-2,4,6-$(CH_3)_3$-3,5-(iPr$_2$PCH$_2$)$_2$C$_6$}(Cl)(CO)$_2$] (**4**) as a pale yellow solid. Formation of **4** results formally from the *cis*-hydride insertion in the exocyclic quinonic double bond accompanied by introduction of two molecules of CO within the coordination sphere while the PPh_3 ligand is lost. This reaction generates a 4-methyl 2,5-cyclohexadienonyl (Scheme 3). A limiting form of this compound, the contribution of which is negligible in the solid state, is a deprotonated form of a σ-arenium species.

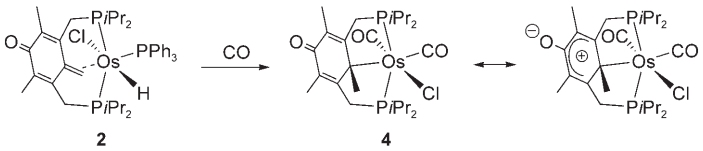

2 **4**

Scheme 3. Formation of **4**.

An X-ray diffraction study was carried out on colorless single crystals of **4** grown from a −30 °C cooled solution of the sample in pentane (Figure 3; selected bond lengths and

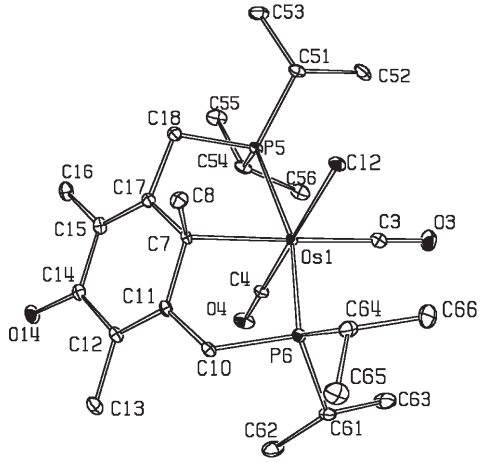

Figure 3. ORTEP view of complex **4** with the thermal ellipsoids at 30% of probability.

angles are given in Table 3). The geometry around the osmium is distorted octahedral. The tridentate PCP fragment is coordinated in a meridional fashion. The chloride and the osmium carbon occupy mutual *cis*-positions, the halide lying on the same side of the Os-PCP plane as the Os-C-*CH$_3$* group. This shows that ligand scrambling occurred under the reaction conditions (namely, migration of the chloride atom in the position *trans* to its original coordination site). The two carbonyl ligands occupy the remaining positions, which are *trans* and *cis* relatively to the Os–C bond. The carbon bound to the osmium atom is sp^3 hybri-

Table 3. Selected bond lengths [Å] and angles [°] of complex **4**.

Os1–C7	2.281(3)	C14–O14	1.243(3)
Os1–C8	3.211(3)	C7–C11	1.491(4)
Os1–C3	1.925(3)	C7–C17	1.495(4)
Os1–C4	1.864(3)	C11–C12	1.354(4)
C3–O3	1.141(4)	C12–C14	1.477(4)
C4–04	1.153(4)	C14–C15	1.471(4)
Os1–Cl2	2.459(1)	C15–C17	1.355(4)
C7–C8	1.546(4)		
P5-Os1-P6	163.67(3)	C7-Os1-C3	177.98(12)
Os1-C7-C8	112.68(19)	C7-Os1-Cl2	92.61(8)
C7-Os1-C4	88.51(12)		

dized (see for example the value of 112.68(19)° for the Os1-C7-C8). The α-methyl group points away from the metal, the large Os1−C8 distance (3.211 Å) excluding the existence of an interaction with the metal center. The Os−C_{alkyl} bond length (Os1−C7 = 2.281(3) Å) is comparable to the analogous distance in the structurally related [Os{(o-$PPh_2C_6H_4)_2$(CH)}(Cl)$(CO)_2$] (2.215(8) Å).[17] The osmium–carbonyl bond lengths are very similar: 1.925(3) and 1.864(3) for **4**, and 1.918(10) and 1.878(10) for [Os{(o-$PPh_2C_6H_4)_2$(CH)}(Cl)$(CO)_2$], for the CO ligands *trans* and *cis* to the Os−C_{PCP} bond, respectively. Bond lengths within the six-membered ring confirm its cyclohexadienonic nature. The average values of the C_i−C_o (C7−C11 and C7−C17) and C_m−C_p (C12−C14 and C14−C15) of 1.493(4) and 1.474(4) Å, respectively, are within the range of single C−C bonds, while the much shorter average C_o−C_m distance (C11−C12 and C17−C15) of 1.354(4) Å) indicates a double bond character. Moreover, the C14−O14 distance of 1.243(3) Å is a typical value for a C=O double bond, comparable to the value observed in **2** and **3**.

In the ^{1}H NMR spectrum, the methyl group in the α-position to the metal resonates as a singlet at $\delta = 1.51$ ppm, while the CH_2P groups appear as a multiplet centered at $\delta =$ 3.36 ppm. The ^{13}C{^{1}H} NMR spectrum comprises notably a singlet at $\delta = 26.61$ ppm for the Os-C-CH_3 moiety, and three low-field resonances: a singlet at $\delta = 184.22$ ppm for the ketonic carbon, and two triplets centered at $\delta = 183.04$ (^2J(P,C) = 6.5 Hz) and 177.24 ppm (^2J(P,C) = 8.0 Hz), for the two carbon monoxide ligands. The infrared spectrum exhibits the expected bands, namely two strong bands of equal intensities at 2006 and 1932 cm^{-1}, corresponding to the ν_{CO} absorptions, as well as a medium intensity absorption at 1600 cm^{-1}, accounting for the ketonic C=O.

Addition of 1.05 equivalents of triflic acid to a solution of **2** causes an immediate color change from orange to deep green and quantitative formation of the cationic methylene arenium species **5a** [Os{4-(CH_2)-1-(OH)-2,6-$(CH_3)_2$-3,5-$(iPr_2PCH_2)_2C_6$}(Cl)(H)(PPh_3)][OTf] (Scheme 4, $X^- = OTf^-$), as indicated by NMR spectroscopy. Addition of NEt_3 to **5a** regenerates quantitatively (by NMR spectroscopy) the quinone methide **2**. Most surprisingly, protonation of **3** also affords **5a** as the only spectroscopically detected complex. Moreover, mixtures of isomeric quinone methides **2** and **3** react with sub-stoichiometric quantities of triflic acid to afford the methylene arenium **5a** as the single detectable species, along with unreacted **3**. The reason for the marked difference in reactivity between **2** and **3** toward protonation is not clear.

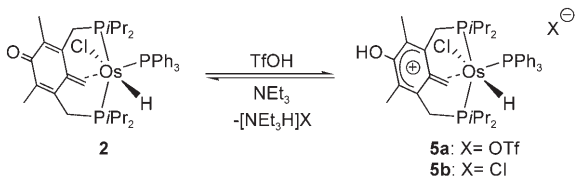

Scheme 4. Interconversion of **2** and **5a**,**b**.

The solid-state structure of **5b**, the chloride derivative of **5a**, obtained following hydrogenolysis of **1** by [$OsCl_2$-$(PPh_3)_3$] is described below. The geometry of the complex is of distorted octahedral type, and is closely related to **2**, with the Os−H lying in the *cis* position from the exocyclic double-bond methylene group. Solution NMR features in $CDCl_3$ of **5b** are consistent with a methylene arenium type structure. The ^{31}P{^{1}H} spectrum consists of a triplet and a doublet (intensities 1:2), respectively, centered at $\delta = -8.03$ and −21.67 ppm, linked by a ^2J(P,P) coupling constant of 15.6 Hz. The C=CH_2 protons resonate at $\delta = 5.28$ ppm as a broad triplet (^3J(H,P) = 6.9 Hz), at higher field than the corresponding signal in **2** ($\delta = 3.76$ ppm). In the related compounds **MA1** and **MA2**,[8] the exocyclic double bond methyl-

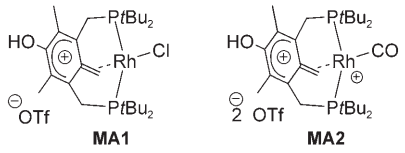

enic protons resonate at $\delta = 4.90$ and 5.20 ppm, respectively. The diastereotopic CH_2P protons give rise to two multiplets, a broad doublet centered at $\delta = 3.40$ ppm and a doublet of virtual triplets at $\delta = 2.58$ ppm, both linked by a geminal coupling constant of 15.8 Hz. The hydride appears at $\delta =$ −10.59 ppm as a doublet of triplets due to the coupling with the two types of phosphorus atoms. A confirmation of the geometry of **5a** is found in the large value of the coupling constant with the PPh_3 phosphorus atom, of 46.9 Hz, similar to the value of 43.1 Hz observed in **2**, while the analogous coupling constant is of 27.7 Hz in **3**.

Regarding the ^{1}H NMR characteristics, the formal protonation of **2** to yield **5a**,**b** is followed by an approximate 1.5 ppm down-field shift of the C=CH_2 signal ($\delta = 3.76$ ppm in **2**, $\delta = 5.28$ ppm in **5a**,**b**, which compares well with the 1.77 ppm shift to lower fields when going from **QM1** to **MA1**), and by an approximate 2.5 ppm downfield shift for the hydride ($\delta = -12.95$ ppm in **2**, $\delta = -10.59$ ppm in **5a**,**b**) (data in the same deuterated solvent). The ^{31}P{^{1}H} NMR spectra are also affected by the structural changes: the chemical shift of the phosphorus atoms in *cis*-position from the coordinated double bond is dramatically affected by the structural changes resulting from the protonation, since the diphosphine ligand gives rise to a doublet at $\delta = -7.83$ ppm in **2** and $\delta = -21.67$ ppm in **5a**,**b**, and the PPh_3, to a triplet at $\delta = -5.58$ ppm in **2** and $\delta = -8.03$ ppm in **5a**,**b**.

The same variations on the chelating diphosphine ^{31}P NMR chemical shifts were observed when comparing **QM1** to **MA1** and **QM2** to **MA2**, with respective deshielding of $\delta =$ 14.12 and 17.01 ppm. The ^{13}C{^{1}H} NMR signals of the coordinated double bond show a downfield shift accompanying the protonation: the C_i atoms resonate at $\delta = 68.38$ and 86.42 ppm in **2** and **5a**,**b**, respectively, and the methylenic carbon atom resonates at $\delta = 29.16$ and 38.91 ppm in **2** and **5a**,**b**, respectively. These two signals follow the same trend

on going from **QM1** to **MA1**. The C_o peak is downfield shifted from $\delta = 152.77$ ppm in **2** to $\delta = 162.52$ ppm in **5a**,**b** while the C_m chemical shift is only slightly affected ($\delta =$ 128.23 ppm in **2** and $\delta = 126.34$ ppm in **5a**,**b**). This is consistent with the partial delocalization of the methylene arenium positive charge in the *ortho*-position. The signal of the C–O carbon atom appears at $\delta = 169.70$ ppm, being shifted upfield by $\delta = 15.84$ ppm, as observed in the case of **MA1** and **MA2**. The effect of the positive charge is also apparent in comparison with the phenolic *C*O chemical shift in **1** ($\delta =$ 150.13 ppm).

Activation of 1 under hydrogen pressure: Under mild hydrogen pressure, $[OsCl_2(PPh_3)_3]$ reacts with **1** at 100 °C in THF to cleanly afford the P-C_{aryl}-P pincer complex **6**, [Os{1-(OH)-2,6-$(CH_3)_2$-3,5-(iPr$_2$PCH$_2$)$_2$C$_6$}(Cl)(H_2)(PPh_3)] (Scheme 5): cleavage of the C–C bond between the aryl ring

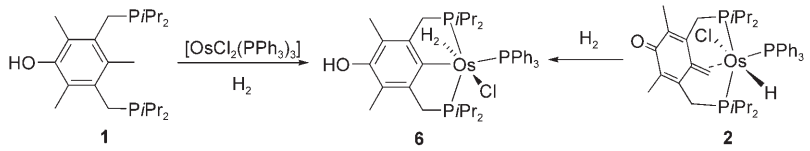

Scheme 5. Formation of the pincer complex **6**.

and the methyl in the 4-position occurs as reported in the related work on the diphosphinic substrate devoid of hydroxyl group.[12] Interestingly, compound **6** can also be prepared from the reaction of **2** with H_2 in toluene at 110 °C.

The formulation of **6** was confirmed by an X-ray diffraction study performed on single crystals of **6** grown from a concentrated benzene solution (Figure 4; selected bond lengths and angles are given in Table 4). The metal-bound hydrogen atoms were located. The geometry of this complex is of a distorted seven-coordinated pentagonal bipyramidal type, with the basal plane formed by the two hydrogen atoms, the chloride, the PPh_3 ligand and the *ipso* carbon of

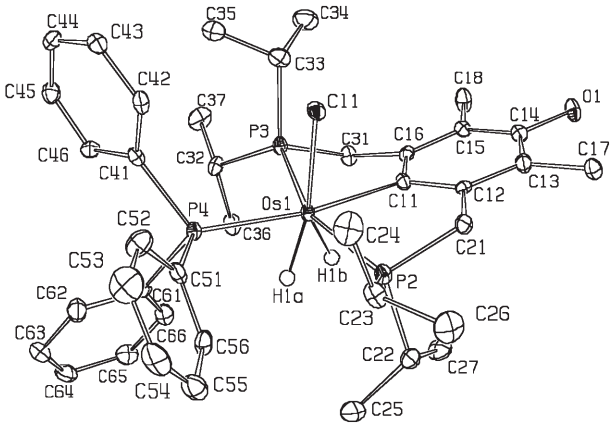

Figure 4. ORTEP view of **6** with the thermal ellipsoids at 30% of probability.

Table 4. Selected bond lengths [Å] and angles [°] of complex **6**.

Os1–P2	2.361(1)	Os1–H1a	1.41(10)
Os1–P3	2.383(2)	Os1–H1b	1.58(6)
Os1–P4	2.422(2)	H1a–H1b	1.336(31)
Os1–Cl1	2.492(2)	C14–O1	1.382(6)
Os1–C11	2.169(5)		
P2-Os1-P3	156.21(4)	H1a-Os1-H1b	53(4)

the PCP framework, while the apical positions are occupied by the PCP phosphinic moieties. This structure is very close to the one described by Jia and co-workers containing a phenyl-substituted PCP ligand.[18] The H1a–H1b distance of 1.336(31) Å classifies complex **6** as a stretched dihydrogen complex.[19] The Os1–C11 distance of 2.169(5) Å is slightly longer than the corresponding distances in the phenyl-substituted compound (2.142(5), 2.146(5) and 2.149(5) Å in the three independent molecules in the unit cell), while the bite angle of the PCP ligand (P2-Os1-P3) of 156.21(4)° is within the range observed in its parent phenyl-substituted compound (155.79(5), 156.89(5) and 158.40(5)°). The C14–O1 distance of 1.382(6) Å is characteristic of a phenolic type bond.

The $^{31}P\{^1H\}$ NMR spectrum of **6** in deuterated benzene consists of a doublet ($\delta = 27.36$ ppm, 2P) and a triplet ($\delta =$ -7.10 ppm, 1P) with $J(P,P) = 10.3$ Hz. The osmium H_2 ligand resonates at $\delta = -12.10$ ppm as a multiplet, which does not resolve upon cooling. The ground state observed in the X-ray structure, which should give rise to two different signals, is not reached. The spectroscopic and structural features similarity to the analogous complex described by Jia, as well as the X-ray diffraction data, allow us to assign the structure of **6** as an elongated dihydrogen complex. As a consequence of the lack of planar symmetry within the (PCP)Os framework, the pincer ligand methylenic protons are diastereotopic and resonate as two doublets of virtual triplets at $\delta = 3.90$ and 3.01 ppm with a geminal coupling constant $^2J(H,H)$ of 15.4 Hz, and a $^vJ(H,P)$ of 3.2 Hz. No coupling with the triphenylphosphine phosphorus atom is observed. The PCP *ipso* carbon resonates at $\delta = 149.24$ ppm as a doublet of multiplets, with a coupling constant of 62.2 Hz, characteristic of coupling with a phosphine ligand *trans* to it. The *C*–O moiety resonates at $\delta = 149.54$ ppm, a chemical shift similar to the one of the analogous signal in **1** ($\delta = 150.13$ ppm).

Lowering the temperature of the reaction between $[OsCl_2(PPh_3)_3]$ and **1** under hydrogen to 80 °C leads to the observation of another compound along with **6**, namely the methylene arenium [Os{4-(CH_2)-1-(OH)-2,6-$(CH_3)_2$-3,5-(iPr$_2$PCH$_2$)$_2$C$_6$}$(Cl)_2$(H)] (**7**), in a ratio of 2:1, respectively, as shown by ^{31}P NMR spectrosco-

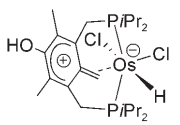

7

py. Formation of complex **7** results formally from the activation of the $ArCH_2$–H bond by the $OsCl_2$ fragment. X-ray data as well as ^1H, $^1H\{^{31}P\}$, and $^{31}P\{^1H\}$ NMR data unequivocally confirm its formulation as a zwitterionic methylene arenium type complex, with a positive charge on the C_6 ring and a negative charge on the metal. Compound **7** is not observed when $OsCl_2(PPh_3)_3$ and **1** react without H_2.

X-ray diffraction studies performed on single crystals of **7** exhibit a distorted octahedral geometry around Os, with the coordinated double bond considered as one ligand (Figure 5; selected bond lengths and angles are given in Table 5). The diphosphine containing ligand is bound to the

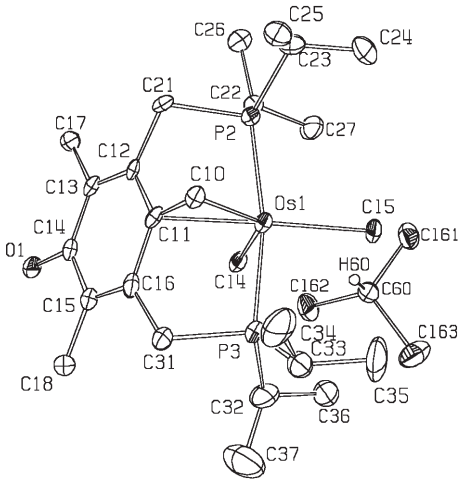

Figure 5. ORTEP view of **7**·$CHCl_3$ with the thermal ellipsoids at 30% of probability.

Table 5. Selected bond lengths [Å] and angles [°] of complex **7**.

Os1–P2	2.358(3)	C14–O1	1.327(13)
Os1–P3	2.353(3)	C11–C12	1.438 (15)
Os1–Cl4	2.485(3)	C11–C16	1.476(15)
Os1–Cl5	2.416(2)	C12–C13	1.380(14)
Os1–C10	2.103(10)	C13–C14	1.443(14)
Os1–C11	2.260(9)	C14–C15	1.433(15)
C10–C11	1.469(15)	C15–C16	1.357(15)
P2-Os1-P3	168.72(9)	Os1-C10-C11	76.2(6)
Cl4-Os1-Cl5	85.02(9)	C10-Os1-Cl5	147.5(3)

osmium in a tetrahapto fashion, with a strong interaction with the coordinated double bond. The hydride ligand, which could not be located, lies in the position *cis* to both the CH_2 group and one of the two chlorides, and *trans* to the other chloride. The C14–O1 distance (1.327(13) Å) is typical of C–O single bonds in aromatic and delocalized systems. The interatomic distances within the ring are characteristic of the methylene arenium structure. Namely, the average C_i–C_o (C11–C12 and C11–C16) bond length (1.457(15) Å) is longer than the average C_o–C_m distance (1.368(14) Å for C12–C13 and C15–C16) and C_m–C_p distance (1.438(14) for C13–C14 and C14–C15). The longer C_m–C_p bond lengths originate from the delocalization of the oxygen electrons pairs, which decreases the double-bond character for the C_m–C_p bonds (Scheme 6). The structural features of the ring system in **7** are similar to those of structurally characterized **MA1**, which bears a similar methylene arenium framework. In this species, alternation between longer C_i–C_o and C_m–C_p average bond lengths (1.444(6) and 1.415(6) Å, respectively) and shorter C_o–C_m average bond length (1.378(6) Å) was also observed, as well as elongated C–O distance (1.338(5) Å).

NMR data indicate that the methylene arenium structure is retained in solution. In deuterated benzene, **7** gives rise to a high field singlet at $\delta = -29.25$ ppm in the $^{31}P\{^1H\}$ NMR spectrum. The osmium-bound methylenic protons resonate at very low field ($\delta = 6.24$ ppm) as a doublet of triplets, while the hydride appears at $\delta = -6.06$ ppm as a triplet of triplets. Both signals are split by the two phosphorus nuclei (respective coupling constants: $^3J(H,P) = 6.1$ Hz and $^2J(H,P) = 11.5$ Hz) and are coupled together ($^3J(H,H) = 2.4$ Hz).

Stirring a solution of **7** in toluene or benzene in the presence of excess PPh_3 leads to the precipitation of the cationic methylene arenium complex $[Os\{4\text{-}(CH_2)\text{-}1\text{-}(OH)\text{-}2,6\text{-}(CH_3)_2\text{-}3,5\text{-}(i Pr_2PCH_2)_2C_6\}(Cl)(H)(PPh_3)]Cl$ (**5b**), as a green solid insoluble in low polarity solvents, moderately soluble in chloroform and THF, and highly soluble in polar solvents. Compound **5b** is the chloride analogue of **5a** presented above (Scheme 4). Single crystals were grown from a concentrated chloroform solution of **5b**, and were submitted to X-rays diffraction studies (Figure 6; selected bond lengths and angles are given in Table 6). The compound is present in the unit cell as discrete cationic and anionic entities. The structure of the osmium cationic complex is similar to that of **2**, regarding the arrangement of the ligands around the metal center. The hydride could not be located.

Several parameters suggest that in the solid-state, **5b** tends to adopt a structural type implying a significant contribution of the benzylic form (Scheme 7) as compared to the zwitterionic methylene arenium **7**.

Indeed, the lengthening of both Os–C distances (Os1–C10 = 2.13(10) Å and Os1–C11 = 2.314(9) Å in **5b** (as compared to 2.103(10) and 2.261(9) in **7**, respectively) indicates a weaker three-center interaction. This is also reflected by

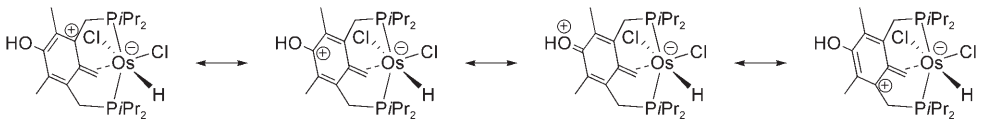

Scheme 6. Resonance forms of **7**.

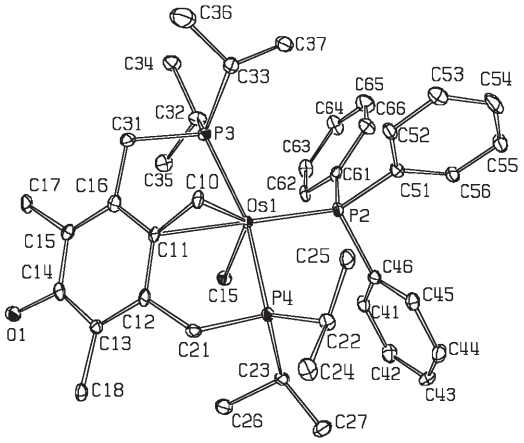

Figure 6. ORTEP view of the cationic fragment of **5b** with the thermal ellipsoids at 30% of probability.

Table 6. Selected bond lengths [Å] and angles [°] of complex **5b**.

Os1–P2	2.371(2)	C14–O1	1.341(13)
Os1–P3	2.393(3)	C11–C12	1.426(14)
Os1–P4	2.397(3)	C11–C16	1.440(14)
Os1–Cl5	2.438(3)	C12–C13	1.387(14)
Os1–C10	2.130(10)	C13–C14	1.420(14)
Os1–C11	2.314(9)	C14–C15	1.400(14)
C10–C11	1.490(14)	C15–C16	1.388(14)
P3-Os1-P4	163.49(9)	Os1-C10-C11	77.2(5)
P2-Os1-Cl5	85.83(9)	C10-Os1-P2	141.2(3)

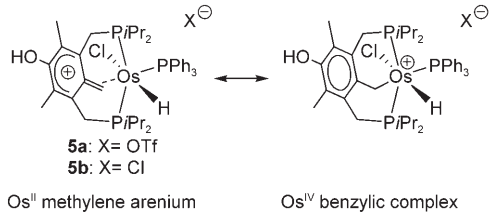

Scheme 7. Limit forms of **5a**,**b**.

the opening of the Os1-C10-C11 angle from 76.2(6)° in **7** to 77.2(5)° in **5b**. The increase of the C10–C11 distance (1.490(14) Å in **5b** compared to 1.469(15) Å in **7**) may indicate that the methylene arenium form plays a smaller part in the actual solid-state structure of **5b** compared with **7**. Along the same line, the intracyclic bond lengths variations are indicative of a comparative re-aromatization of the cyclic delocalized system, as shown in the averaged homologous C–C distances in **5b**: 1.433(15) Å for the C_i–C_o distances (C11–C12 and C11–C16), 1.387(14) Å for the C_o–C_m distances (C12–C13 and C15–C16), and 1.410(14) Å for the C_m–C_p distances (C13–C14 and C14–C15), to be compared to 1.457(15), 1.368(14) and 1.438(14) Å, respectively, in **7**. Accordingly, the longer C14–O1 distance of 1.341(13) Å (1.327(13) Å in **7**) is indicative of less pronounced delocalization of the oxygen electrons into the delocalized cyclic system in **7** compared to **5a**. The decreased participation of the methylene arenium character in going from **7** to **5b** may be due to the steric pressure exerted by the rather bulky triphenylphosphine ligand, which pushes away the isopropyl substituents on the chelating ligand (see the bite angles of 168.72(9) and 163.49(9)° in **7** and **5b**, respectively), thus moving away the aromatic system from the metal, and thereby reducing the interaction with the double bond.

The structural changes accompanying the protonation of **2** into **5b** are similar to that observed when switching from **QM1** to **MA1**. Indeed, in these closely related pairs the CH_2–C_i bond length increases from 1.453(7) Å in **2** to 1.490(14) Å in **5b**, to be compared to 1.441(8) Å in **QM1** and 1.452(6) Å in **MA1**. A similar tendency is observed for the C–O distance, which increases upon protonation from 1.254(7) Å in **2** to 1.341(13) Å in **5b**, while it rises from 1.239(6) in **QM1** to 1.338(5) Å in **MA1**.

Changes within the cyclic system are comparable between the two pairs: a switch to the methylene arenium structure induces shortening of the average C_i–C_o and C_m–C_p bond lengths within the **2**/**5b** pair (from 1.457(15) to 1.444(6) Å, and from 1.438 (14) to 1.415(16) Å, respectively), as within the **QM1**/**MA1** pair (from 1.472(6) to 1.433(15) Å, and from 1.466(7) to 1.410(14) Å, respectively). This is accompanied by the lengthening of the average C_o–C_m distance, which increases from 1.344(7) Å in **2** to 1.387(14) Å in **5b**, to be compared to 1.351(8) Å in **QM1** and 1.378(6) Å in **MA1**.

Thus, introduction of PPh_3 onto the metal leads to partial rearomatization and to a slight metal slippage toward the methylene group, consistent with a stronger participation of the benzylic form. This contrasts with the absence of such a phenomenon when comparing **MA1** and **MA2**.[8b]

The ^1H and ^{31}P NMR spectroscopic features of **5b** and **5a** are identical. When comparing **7** and **5a**,**b**, the hydride signal in the ^1H NMR spectrum is dramatically affected by the change of one of its *cis* ligands from Cl^- to PPh_3, exhibiting a 4.5 ppm downfield shift ($\delta = -10.59$ ppm in **5b**, compared to $\delta = -6.06$ ppm in **7**). This could be due to the existence of an interaction between the hydride and an *ortho*-proton of the triphenylphosphine, as observed in the solid-state structure of **2** and **5b**.

Compounds **5a**,**b** can be viewed as cationic derivatives of **7**. Their formation formally results from the displacement of the chloride *trans* to the coordinated double bound in **7** by a triphenylphosphine ligand. The existence of an equilibrium between the neutral species **7** and the corresponding charge-separated ion pair would account for the formation of the cationic derivative **7**. The ionic intermediate being trapped by free PPh_3, the balance would be shifted towards the formation of **7** with the precipitation as a driving force (Scheme 8).

Discussion

The various reactivity patterns allow us to propose a reaction scheme accounting for the formation of quinone me-

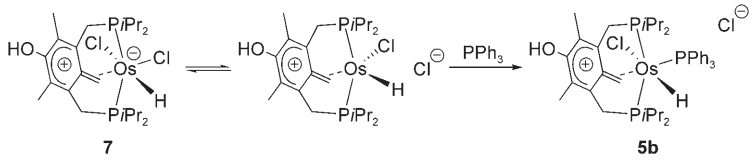

Scheme 8. Proposed formation mechanism for **5b**.

thide derivatives **2** and **3** from $[OsCl_2(PPh_3)_3]$ and **1** in the presence of NEt_3, in which the various intermediates have been isolated and the reactions connecting them have been elucidated (Scheme 9). Coordination of **1** to osmium followed by C–H activation generates the zwitterionic methylene arenium **7** after PPh_3 elimination. Subsequent chloride substitution by a triphenylphosphine ligand affords the cationic methylene arenium **5b**, which is deprotonated to form the quinone methide **2**. The thus generated triethylammonium chloride catalyzes the isomerization of **2** into a mixture of **2** and **3**.

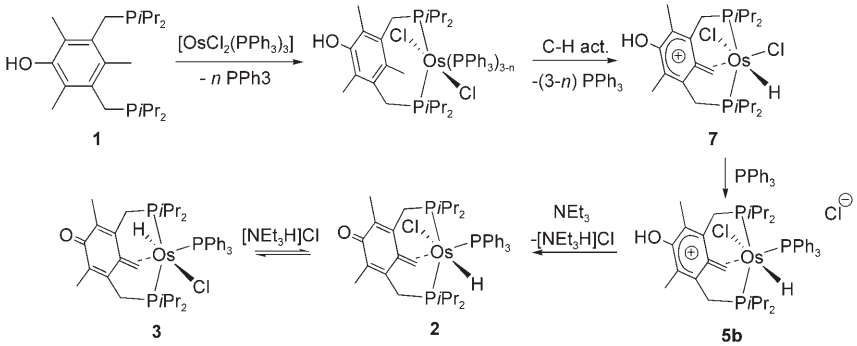

Scheme 9. Reaction pathway leading to the formation of the quinone methides **2** and **3**.

The observation of **7** in the hydrogenolysis reaction mixture obtained at 80 °C is an indication that in this complex the C–C bond cleavage is not favored. The fact that no other species besides **7** and the C–C cleaved **6** is observed under conditions suitable for the formation of quinone methides **2** and **3** (from which **6** can be formed under H_2 pressure) or methylene arenium **5b**, is an indication that these species can rapidly evolve to the C–C cleaved compound. This may imply that in this system, chloride substitution by triphenylphosphine assists C–C activation. This is also reflected in the comparison of the solid-state structures of **7** and **5b**: in **5b**, a higher benzylic contribution is observed relative to **7**. This may imply that the species resulting from hydride insertion into the double bond of **7** would be of the methyl arenium type, while in the case of **5b**, this would result in an unsaturated system which may form an agostic C–C bond, thus allowing metal insertion (Scheme 10).[20,21]

The formation of **6** from both **2** and **1**/$[OsCl_2(PPh_3)_3]$ in the presence of hydrogen may be related to these observations. Starting from **2**, the plausible first step is the abovementioned OsH insertion into the exocyclic double bond affording intermediate **A**, with a PCP framework analogous to the one observed in the bis-carbonyl derivative **4** (Scheme 11).

Different hypotheses may then be proposed regarding the mechanistic pathway leading to **6**: 1) electron transfer from the osmium center to the cyclohexadienonic π system, thus re-aromatized to a phenate system with the C_{Ar}–CH_3 bond potentially involved in an agostic interaction, and consecutive C–C bond activation to afford a (PCP) phenate–methyl species which undergoes hydrogenolysis of the Os–CH_3 bond; or 2) α-methyl transfer to the metal preceded or followed by H_2 addition and subsequent methane elimination. The formally obtained species are the zwitterionic hydridochlorophenate in the case of 1), or the mesomeric hydridochloro osmaquinone[22] in the case of 2). These may tautomerically rearrange into $[Os(PCP)(Cl)(PPh_3)]$. This species reacts in turn with H_2 to afford complex **6**, as observed in the reported chemistry of the non-hydroxyl-substituted complex.[12] These features contrast with the rhodium quinone methides chemistry, in which facile C–C cleavage and methyl group migration are involved.[8]

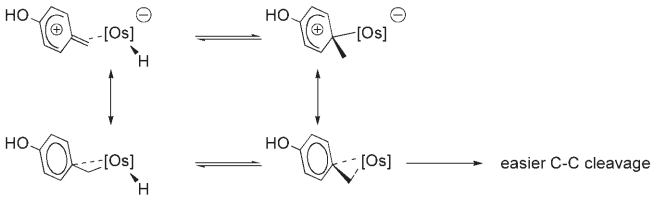

Scheme 10. Hydride insertion in the methylene arenium and benzylic structures.

Conclusion

In summary, isomeric quinone methides were obtained by the reaction of $[OsCl_2(PPh_3)_3]$ with a phenolic diphosphine ligand under mild conditions. These complexes proved to be stable in alcoholic medium, in marked contrast to the free quinone methides, but in accordance to the related chemistry of rhodium and palladium derivatives. Intermediates in their formation were isolated, namely neutral and cationic methylene arenium species, thus shedding light on the mechanistic pathway leading to the quinone methides. While the origin of these species stems from osmium-mediated C–H bond activation of the methyl group located between the phosphinic arms, C–C bond activation was achieved under mild H_2 pressure both by direct activation of the phenolic substrate, and from the quinone methides, resulting in the

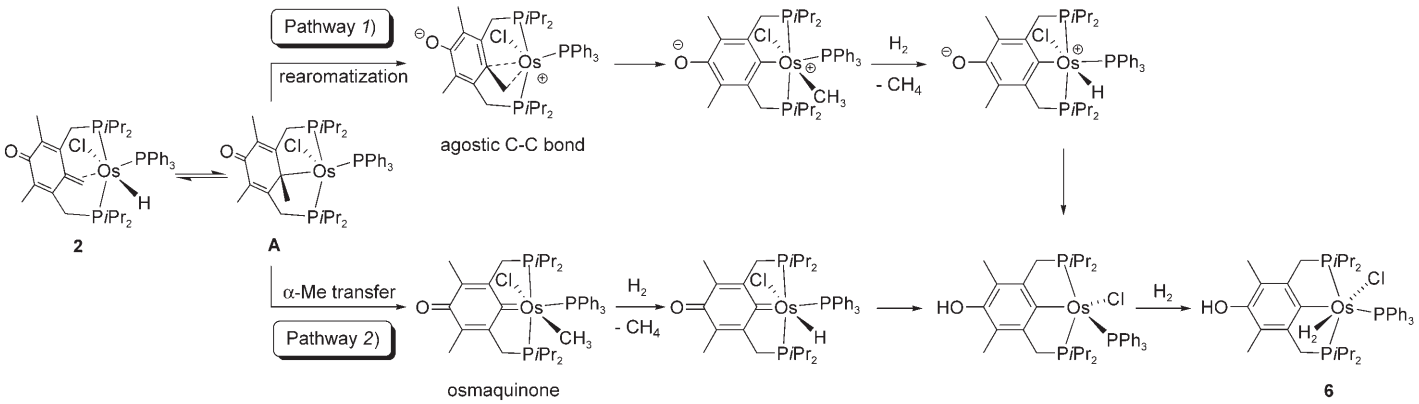

Scheme 11. Proposed mechanism for the formation of **6**.

formation of a PCP pincer-type dihydrogen adduct. These results complement those obtained in our group on the interesting family of η^2-quinonoid compounds, and contribute to the development of the field of metal-induced aromatic system pertubation.

Experimental Section

General procedures: All reactions were carried out under an inert atmosphere in a glove box or using standard Schlenk techniques. Solvents were dried, distilled, and degassed before use. $[OsCl_2(PPh_3)_3]$ was prepared following literature procedures.[23] ^{1}H, ^{31}P{^{1}H} and ^{13}C{^{1}H} NMR spectra were recorded on a Bruker AMX400 spectrometer at 400, 162 and 100 MHz, respectively, or on a Bruker DPX250 spectrometer at 250, 101 and 62 MHz, respectively. ^{1}H and ^{13}C chemical shifts are reported in ppm downfield from TMS and referenced to the residual proton impurities in the solvent and all-[D] solvent peaks, respectively. ^{31}P NMR chemical shifts are in ppm downfield from H_3PO_4 and referenced to an external 85% H_3PO_4 sample. All measurements were performed at 20°C. Assignments of ^{1}H and ^{13}C{^{1}H} NMR signals were done with ^{1}H-{^{31}P} and ^{13}C-DEPT-135 NMR, respectively. Infrared spectra were collected on a Nicolet Protégé 460 spectrometer. Elemental analyses were carried out by H. Kolbe, Mülheim an der Ruhr, Germany. ORTEP drawings were generated by Ortep-3 1.074.[24]

2,4,6-$(CH_3)_3$-3,5-$(iPr_2PCH_2)_2C_6OH$ (1): In the glove box, a solution of diisopropylphosphine (5.664 g, 48 mmol) in acetone (75 mL) was added to a solution of 3,5-bis(bromomethyl)-2,4,6 trimethylphenol (6.44 g, 20 mmol, prepared following the procedure of van der Made[25]) in acetone (75 mL). After being stirred at room temperature for an hour, during which time a white precipitate formed, the reaction mixture was taken out of the dry box, refluxed under argon for 4 h and stirred overnight at room temperature. Pentane was then added, and the liquid phase was decanted off. The solid was washed with a fresh portion of pentane, dissolved in 100 mL degassed water, and added to a degassed solution of 30 g of sodium acetate in water (100 mL). Three successive extractions with methylene chloride were carried out, and the combined organic phase was dried over sodium sulfate and filtered into a dry nitrogen-flushed flask. Volatiles were evaporated to dryness, washed with diethyl ether and pentane and dried under vacuum to afford 6.03 g of a colorless solid. (Yield: 76%). ^{1}H NMR ($CDCl_3$): $\delta = 4.58$ (br s, 1H; OH), 2.88 (d, ^2J(H,P) = 1.9 Hz, 4H; $ArCH_2P$), 2.41 (s, 3H; Ar-CH_3), 2.28 (s, 6H; Ar-CH_3), 1.80 (m, 4H; CH *i*Pr), 1.12 (m, 12H; CH_3 *i*Pr), 1.01 ppm (m, 12H; CH_3 *i*Pr); ^{31}P{^{1}H} NMR ($CDCl_3$): $\delta = 8.21$ ppm; ^{13}C{^{1}H} NMR ($CDCl_3$): $\delta = 150.13$ (*C*-OH), 134.67 (2 C_{Ar}), 126.84 (1 C_{Ar}), 119.28 (2 C_{Ar}), 24.44 (d, ^1J(C,P) = 21.8 Hz, $ArCH_2P$), 23.22 (d, ^1J(C,P) = 15.5 Hz, CH *i*Pr), 19.69 (s, CH_3 *i*Pr), 19.49 (d, ^2J(C,P) = 3.05 Hz, CH_3 *i*Pr), 18.07 (t, ^4J(C,P) = 6.5 Hz, 4-CH_3-Ar), 13.41 ppm (d, ^4J(C,P) = 6.0 Hz, 2,6-CH_3-Ar); elemental analysis calcd (%) for $C_{23}H_{42}OP_2$: C 69.67, H 10.68; found: C 69.60, H: 10.74.

Synthesis of the osmium quinone methides 2 and 3: Compound **1** (160 mg, 0.404 mmol) and NEt_3 (0.2 mL, 1.45 mmol) dissolved in benzene (4 mL) were added to a suspension of $[OsCl_2(PPh_3)_3]$ (420 mg, 0.401 mmol) in benzene (4 mL). The reaction mixture was heated for 4 h at 60°C, turning to dark orange. After cooling to room temperature and filtration on a Celite pad, the filtrate was concentrated to about 2 mL, and pentane (5 mL) was added. The precipitate was separated by decantation, washed with pentane and dried under vacuum. This procedure afforded a mixture of **2** and **3** in 2:1 ratio. Yield: 268 mg (76%). Fractional crystallization from toluene/pentane (or toluene/diethyl ether) at −30°C afforded analytically pure **2**. Extraction of the **2**–**3** mixture with pentane and standing of the solution for 4 days afforded crystals of **3**.

[Os{4-(CH_2)-1-(O)-2,6-$(CH_3)_2$-3,5-$(iPr_2PCH_2)_2C_6$}(Cl)(H)(PPh_3)] (**2**): ^{1}H NMR ($CDCl_3$): $\delta = 7.96$ (m, 6H; H_o PPh_3), 7.33 (m, 9H; PPh_3), 3.76 (dt, ^3J(H,P) = 1.4 Hz, ^3J(H,P) = 6.70 Hz, 2H; $OsCH_2$), 2.87 (dvt, ^2J(H,H) = 15.9 Hz, $^2J_{HP}$ = 4.5 H; 2H; C*H*HP), 2.41 (dvt, ^2J(H,H) = 15.7 Hz, ^2J(H,P) = 4.3 Hz, 2H; CH*H*P), 2.00 (s, 6H; Ar-CH_3), 1.98 (m, 2H; CH *i*Pr), 1.03 (m, 6H; CH_3 *i*Pr), 0.97 (m, 20H; 3 CH_3 *i*Pr + CH_3 *i*Pr), −12.95 ppm (dt, ^2J(H,P) = 43.1 Hz, ^2J(H,P) = 9.8 Hz, 1H; OsH); ^{31}P{^{1}H} NMR ($CDCl_3$): $\delta = -5.58$ (t, ^2J(P,P) = 16.1 Hz, 1P, PPh_3), −7.83 ppm (d, ^2J(P,P) = 16.1 Hz, 2P, PCP); ^{13}C{^{1}H} NMR ($CDCl_3$): $\delta = 185.77$ (s, *C*=O), 152.77 (m, C_m *PCP*), 138.72 (d, $^1J_{PC}$ = 44.1 Hz, C_i PPh_3), 135.24 (m, PPh_3), 129.67 (m, PPh_3), 128.23 (t, $^1J_{PC}$ = 4.8 Hz, C_o *PCP*), 127.26 (m, PPh_3), 68.38 (dt, ^2J(C,P) = 19.5 Hz, 3.6 Hz, *C*=CH_2), 29.16 (br s, C=CH_2), 24.56 (vt, ^vJ(C,P) = 11.6 Hz, CH *i*Pr), 22.43 (vt, ^vJ(C,P) = 10.6 Hz, CH *i*Pr), 21.41 (s, CH_3), 20.91 (s, CH_3), 19.81 (br s, CH_3), 18.17 (s, CH_3), 17.46 (td, J(C,P) = 11.3 Hz, 1.3 Hz, *C*H_2P), 13.51 ppm (s, CH_3); IR (film): $\tilde{\nu} = 2167$ (m, $\nu_{Os\text{-}H}$), 1629 cm^{-1} (s, ν_{CO}); elemental analysis calcd (%) for $C_{41}H_{56}ClOOsP_3$: C 55.74, H 6.39; found: C 55.76, H: 6.69.

[Os{4-(CH_2)-1-(O)-2,6-$(CH_3)_2$-3,5-$(iPr_2PCH_2)_2C_6$}(Cl)(H)(PPh_3)] (**3**): ^{1}H NMR (C_6D_6): $\delta = 8.13$ (m, 6H; H_o PPh_3), 6.98 (m, 9H; PPh_3), 3.64 (dt, ^3J(H,P) = 2.7 Hz, $^3J_{HP}$ = 7.2 Hz, 2H; $OsCH_2$), 2.61 (d, ^2J(H,H) = 16.2 Hz, 2H; C*H*HP), 2.25 (s, 6H; Ar-CH_3), 2.00 (dt, ^2J(H,H) = 16.2 Hz, $^2J_{HP}$ = 4.3 Hz, 2H; CH*H*P), 1.87 (m, 2H; CH *i*Pr), 1.70 (m, 2H; CH *i*Pr), 1.07 (m, 6H; CH_3 *i*Pr), 1.00 (m, 6H; CH_3 *i*Pr), 0.87 (m, 6H; CH_3 *i*Pr), 0.41 (m, 6H; CH_3 *i*Pr), −13.60 ppm (dt, ^2J(H,P) = 27.7 Hz, ^2J(H,P) = 12.0 Hz, 1H; OsH); ^{1}H NMR ($CDCl_3$): $\delta = 7.94$ (m, 6H; H_o PPh_3), 7.33 (m, 9H; PPh_3), 3.49 (dt, ^3J(H,P) = 2.6 Hz, ^3J(H,P) = 7.2 Hz, 2H; $OsCH_2$), 2.91 (d, ^2J(H,H) = 16.2 Hz, ^2J(H,P) = 3.7 Hz, 2H; C*H*HP), 2.23 (dt, ^2J(H,H) = 16.1 Hz, ^2J(H,P) = 4.4 Hz, 2H; CH*H*P), 2.02 (m, 2H; CH *i*Pr), 1.97 (s, 6H; Ar-CH_3), 1.70 (m, 2H; CH *i*Pr), 1.05 (m, 6H; CH_3 *i*Pr), 0.90 (m, 6H; CH_3 *i*Pr), 0.79 (m, 6H; CH_3 *i*Pr), 0.61 (m, 6H; CH_3 *i*Pr), −13.69 ppm (dt, ^2J(H,P) = 28.3 Hz, ^2J(H,P) = 12.1 Hz, 1H; OsH); ^{31}P{^{1}H} NMR (C_6D_6): $\delta = -5.49$ (d, 2P, ^2J(P,P) = 15.3 Hz, PCP), −11.54 ppm (t, 1P, ^2J(P,P) = 15.3 Hz, PPh_3); ^{31}P{^{1}H} NMR ($CDCl_3$): $\delta = -4.61$ (d, 2P, ^2J(P,P) = 15.0 Hz, PCP), −8.59 ppm (t, 1P, ^2J(P,P) = 15.0 Hz, PPh_3); ^{13}C{^{1}H}

NMR ($CDCl_3$): $\delta = 184.87$ (s, *C*=O), 159.48 (m, C_m *PCP*), 135.58 (d, C_o PPh_3), 129.76 (d, C_p, PPh_3), 127.26 (m, PPh_3), 124.08 (t, $^1J(C,P) = 4.7$ Hz, C_o *PCP*), 65.69 (m, *C*=CH_2), 38.78 (m, C=*C*H_2), 27.55 (vt, $^vJ(C,P) = 12.9$ Hz, CH *i*Pr), 26.51 (vt, $^vJ_{PC} = 10.6$ Hz, CH *i*Pr), 20.36 (t, $^vJ(C,P) = 12.1$ Hz, CH_2P), 19.12 (s, CH_3), 18.65 (s, CH_3), 18.48 (s, CH_3), 13.60 ppm (s, CH_3); IR (film): $\tilde{\nu} = 1615$, 1583 cm^{-1} (s, quinone); elemental analysis calcd (%) for $C_{41}H_{56}ClOOsP_3$: C 55.74, H 6.39; found: C 55.70, H: 6.47.

[Os{1-(O)-2,4,6-$(CH_3)_3$-3,5-(*i*$Pr_2PCH_2)_2C_6$}(Cl)$(CO)_2$] (4): In a Fischer–Porter bottle, an orange solution of **2** (50 mg, 0.057 mmol) in THF (5 mL) was stirred under 2 bar of CO at 80 °C for 10 h. After cooling to room temperature, the solution was evaporated to dryness to yield a pale yellow solid. NMR analysis showed quantitative formation of **4**. Redissolving the reaction mixture in pentane (2 mL) and cooling this solution at −30 °C led to the formation of colorless crystals of **4** (15 mg, isolated yield: 39 %). ^{1}H NMR ($CDCl_3$): $\delta = 3.36$ (m, 4H; CH_2P), 3.16 (m, 2H; CH *i*Pr), 2.16 (m, 2H; CH *i*Pr), 2.02 (s, 6H; cyclohexadienone CH_3), 1.51 (s, 3H; Os-CR_2-CH_3), 1.42 (m, 6H; CH_3 *i*Pr), 1.38 (m, 12H; CH_3 *i*Pr), 1.29 ppm (m, 6H; CH_3 *i*Pr); ^{31}P{^{1}H} NMR ($CDCl_3$): $\delta = 13.78$ ppm (s, PCP); ^{13}C{^{1}H} NMR ($CDCl_3$): $\delta = 184.87$ (R_2C=O), 181.61 (t, $^2J(C,P) = 6.5$ Hz, Os*C*O), 176.08 (t, $^2J(C,P) = 8.0$ Hz, Os*C*O), 164.94 (t, $^2J(C,P) = 4.0$ Hz, C quat. PCP), 123.97 (t, $J(C,P) = 5.5$ Hz, , C quat. PCP), 45.61 (s, Os-C PCP), 29.73 (vt, $^vJ(C,P) = 14.7$ Hz, CH_2P), 26.59 (OsCCH_3), 25.49 (vt, $^vJ(C,P) = 13.3$ Hz, CH *i*Pr), 23.32 (vt, $^vJ(C,P) = 12.5$ Hz, CH *i*Pr), 20.08 (CH_3), 19.61 (CH_3), 19.09 (CH_3), 17.77 (CH_3), 12.59 ppm (CH_3); IR (film): $\tilde{\nu} = 2006$ (s, ν_{CO}), 1932 (s, ν_{CO}), 1623 (w), 1600 cm^{-1} (m, C=O); elemental analysis calcd (%) for $C_{25}H_{41}ClO_3OsP_2$: C 44.34, H 6.10; found: C 44.40, H: 6.17.

Methylene arenium derivatives [Os{4-(CH_2)-1-(OH)-2,6-$(CH_3)_2$–3,5-(*i*$Pr_2PCH_2)_2C_6$}(H)(Cl)(PPh_3)]X (5)

Synthesis of ***5a*** *($X^- = OTf^-$)*: Triflic acid (1.05 equiv, 0.042 mmol) in dioxane (0.084 mL) was added to a solution of **2** (35 mg, 0.040 mmol) in benzene (2 mL). A green precipitate immediately formed, which was filtered, washed with benzene and dried under vacuum. Yield: 39 mg (95 %). Elemental analysis calcd (%) for $C_{42}H_{57}ClF_3O_4OsP_3S$: C 47.87, H 5.31; found: C 47.78, H: 5.38.

Synthesis of ***5b*** *($X^- = Cl^-$)*: In a Fischer–Porter bottle, [$OsCl_2(PPh_3)_3$] (50 mg, 0.047 mmol) and **1** (19 mg, 0.048 mmol) were dissolved in THF (5 mL). The solution was pressurized with 2.5 bar of hydrogen and heated at 80 °C for 16 h. The resulting pale green turbid solution was filtered on a Celite pad, evaporated to dryness, redissolved in toluene (5 mL) and vigorously stirred for 30 min. A green precipitate of **5b** formed, which was separated by filtration, washed with toluene (2×2 mL) and dried under vacuum. Yield: 11 mg (25 %). Letting a concentrated solution of **5b** in chloroform stand led to the formation of X-ray quality single crystals. ^{1}H NMR ($CDCl_3$): $\delta = 7.90$ (m, 6H; H_o PPh_3), 7.41 (m, 9H; H_m + H_p PPh_3), 5.28 (br t, $^3J(H,P) = 6.9$ Hz, 2H; $OsCH_2$), 3.40 (br d, $^2J(H,H) = 15.8$ Hz, 2H; CH*H*P), 2.58 (dvt, $^2J(H,H) = 15.8$ Hz, $^vJ_{HP} = 4.3$ Hz, 2H; C*H*HP), 2.43 (s, 6H; Ar-CH_3), 1.68 (m, 2H; CH *i*Pr), 1.47 (m, 2H; CH *i*Pr), 1.04 (m, 18H; CH_3 *i*Pr), 0.64 (m, 6H; CH_3 *i*Pr), −10.59 ppm (dt, $^2J(H,P) = 46.9$ Hz, $^2J_{HP} = 9.7$ Hz, 1H; OsH); ^{31}P{^{1}H} NMR ($CDCl_3$): $\delta = -8.03$ (t, $^2J(P,P) = 15.6$ Hz, PPh_3), −21.67 ppm (d, $^2J(P,P) = 15.6$ Hz, PCP); ^{13}C{^{1}H} NMR (CD_3OD): $\delta = 169.70$ (s, *C*-O), 162.52 (m, C_m *PCP*), 137.42 (d, $^1J(C,P) = 52.3$ Hz, C_i PPh_3), 136.64 (d, $J(C,P) = 8.4$ Hz, PPh_3), 132.20 (d, $J(C,P) = 2.3$ Hz, PPh_3),129.10 (d, $J(C,P) = 9.7$ Hz, PPh_3), 126.34 (t, $^2J(C,P) = 4.7$ Hz, C_o PCP), 86.42 (dm, $^2J(C,P) = 13.9$ Hz, *C*=CH_2), 38.91 (br s, C=*C*H_2), 27.29 (vt, $^vJ(C,P) = 12.0$ Hz, CH *i*Pr), 23.29 (vt, $^vJ(C,P) = 11.0$ Hz, CH *i*Pr), 21.66 (s, CH_3), 21.61 (s, CH_3), 20.38 (s, CH_3), 20.09 (vt, $^vJ(C,P) = 10.2$ Hz, CH_2P), 18.84 (s, CH_3), 13.43 ppm (s, CH_3); elemental analysis calcd (%) for $C_{42}H_{58}Cl_5F_3OOsP_3$ (**5b**.$CHCl_3$): C 48.54, H 5.62; found: C 47.85, H: 5.64.

[Os{1-(OH)-2,6-$(CH_3)_2$-3,5-(*i*$Pr_2PCH_2)_2C_6$}(Cl)$(H_2)(PPh_3)$] (6)

Method A: In a Fischer–Porter bottle, a solution of **2** (36 mg, 0.041 mmol) in toluene (6 mL) was stirred under 3.5 bar of H_2 at 110 °C. ^{31}P{^{1}H} NMR analysis of the crude mixture showed a conversion of 6 % after 30 min. The reaction mixture was re-pressurised with hydrogen, and heating was continued for 16 h. After cooling to room temperature, the pale yellow solution was evaporated to about 0.5 mL and stored at −30 °C. A white solid precipitated, which was separated by decantation, and washed with Et_2O. Yield: 27 mg (76 %).

Method B: In a Fischer–Porter bottle, [$OsCl_2(PPh_3)_3$] (266 mg, 0.254 mmol) and **1** (150 mg, 0.378 mmol) in THF (10 mL) were stirred under 2.5 bar of H_2 at 100 °C for 14 h. After cooling to room temperature, the reaction mixture was filtered over a Celite pad. The filtrate was evaporated to dryness, and the solid residue was vigorously stirred over ethanol (5 mL) for 30 min. The white solid was separated from the supernatant by decantation, washed with ethanol (2×2 mL) and dried under vacuum. Yield: 163 mg (74 %). ^{1}H NMR (C_6D_6): δ 8.10 (m, 6H; PPh_3), 7.04 (m, 9H; PPh_3), 4.09 (br s, 1H; OH), 3.90 (dvt, $^2J(H,H) = 15.4$ Hz, $^vJ(H,P) = 3.2$ Hz, 2H; ArC*H*HP), 3.01 (dvt, $^2J(H,H) = 15.4$ Hz, $^vJ(H,P) = 3.4$ Hz, 2H; ArCH*H*P), 2.22 (s, 6H; Ar-CH_3), 2.13 (m, 2H; CH *i*Pr), 1.42 (m, 2H; CH *i*Pr), 1.02 (m, 6H; CH_3 *i*Pr), 0.79 (m, 6H; CH_3 *i*Pr), 0.73 (m, 6H; CH_3 *i*Pr), 0.72 (m, 6H; CH_3 *i*Pr), −12.10 ppm (m, 2H; $Os(H)_2$); ^{31}P{^{1}H} NMR (C_6D_6): $\delta = 27.36$ (d, $^2J(P,P) = 10.3$ Hz, PCP), −7.10 ppm (t, $^2J(P,P) = 10.3$ Hz, PPh_3); ^{13}C{^{1}H} NMR (C_6D_6): 149.54 (s, C-OH), 149.24 (dm, $^2J_{PC} = 62.2$ Hz, C_i Ar PCP), 142.93 (t, $J(C,P) = 7.4$ Hz, C_o Ar PCP), 140.60–115.74 (C Ar), 37.30 (dvt, $^vJ(C,P) = 16.8$ Hz, $^3J_{PC} = 6.1$ Hz, $ArCH_2P$), 25.27 (vt, $^vJ(C,P) = 13.3$ Hz, CH *i*Pr), 24.21 (vt, $J(C,P) = 10.8$ Hz, CH *i*Pr), 20.20 (s, CH_3), 19.60 (CH_3), 19.01 (CH_3), 18.53 ppm (CH_3), 14.96 (CH_3); elemental analysis calcd (%) for $C_{40}H_{56}ClOOsP_3$: C 55.13, H 6.48; found: C 55.66, H: 6.52.

[Os{4-(CH_2)-1-(OH)-2,6-$(CH_3)_2$-3,5-(*i*$Pr_2PCH_2)_2C_6$}$(Cl)_2$(H)] (7): In a Fischer–Porter bottle, [$OsCl_2(PPh_3)_3$] (50 mg, 0.047 mmol) and **1** (19 mg, 0.048 mmol) were dissolved in THF (5 mL). The solution was pressurized with 2.5 bar of hydrogen and heated at 80 °C for 16 h. The resulting pale green turbid solution was filtered on a Celite pad. ^{31}P{^{1}H} NMR spectrum of an aliquot of the solution showed the presence of **6** and **7** in a 2:1 ratio, respectively, along with free triphenylphosphine. The solution was evaporated to dryness and the residue was washed with pentane (3× 1 mL). The remaining solid was dissolved in a 1:1 toluene:pentane solvent mixture (5 mL) and cooled overnight at −30 °C, leading to precipitation of a green material. Washing with toluene (0.5 mL) resulted in formation of 12 mg of a 1:2 mixture of **6** and **7**, respectively. Further separation attempts were not successful. Slow evaporation of a solution of the mixture in chloroform allowed the formation of a single crystal of **7**, suitable for X-ray diffraction studies. ^{1}H NMR ($CDCl_3$): $\delta = 8.66$ (s, large, 1H; OH), 6.24 (dt, $^3J(H,H) = 2.4$ Hz, $^3J(H,P) = 6.1$ Hz, 2H; $OsCH_2$), 3.41 (dvt, $^2J(H,H) = 14.9$ Hz, $^vJ(H,P) = 4.6$ Hz, 2H; ArCH*H*P), 2.85 (m, 2H; CH *i*Pr), 2.64 (dvt, $^2J(H,H) = 14.6$ Hz, $^vJ(H,P) = 3.6$ Hz, 2H; ArC*H*HP), 2.36 (s, 6H; Ar-CH_3), 1.80 (m, 2H; CH *i*Pr), 1.76 (m, 6H; CH_3 *i*Pr), 1.33 (m, 6H; CH_3 *i*Pr), 1.29 (m, 6H; CH_3 *i*Pr), 1.00 (m, 6H; CH_3 *i*Pr), −6.06 ppm (tt, $^3J(H,H) = 2.4$ Hz, $^2J(H,P) = 11.5$ Hz, H, OsH); ^{31}P{^{1}H} NMR ($CDCl_3$): $\delta = -29.25$ ppm (s, PCP).

X-ray structure determination and refinement of complexes 2, 3, 4, 5b, 6, and 7: The crystals were coated with mineral oil, mounted in a nylon loop and flash frozen in a cold nitrogen stream (120 K) on a Nonius KappaCCD diffractometer with $Mo_{K\alpha}$ radiation ($\lambda = 0.71071$ Å). Accurate unit cell dimensions were obtained from 20° of data. The data were processed with the Denzo-Scalepack package.[26] The structures were solved by direct methods (SHELXS-97[27]) and refined by full-matrix least-squares (SHELXL-97[27]). Idealized hydrogen atoms were placed and refined in the riding mode, with the exception of H1 in compound **2**, and H1a and H1b of compound **6** which were located in the difference electron density and refined independently. Crystal data for compounds **2**, **3**, **4**, **5b**, **6**, and **7** are given in Table 7. CCDC-620587 (**2**), CCDC-620584 (**3**), CCDC-620585 (**4**), CCDC-620583 (**5b**), CCDC-620586 (**6**) and CCDC-620582 (**7**) contain the supplementary crystallographic data for this paper. These data can be obtained free of charge from the Cambridge Crystallographic Data Centre via www.ccdc.cam.ac.uk/data_request/cif.

Acknowledgements

This work was supported by the Israel Science Foundation, the Minerva Foundation and the Helen and Martin Kimmel Center for Molecular

Table 7. Experimental crystallographic data for complexes **2**, **3**, and **4**.

	2	**3**	**4**	**5b**	**6**	**7**
color	yellow-orange	orange	yellow	green	colorless	green
formula	$C_{42}H_{57}Cl_4OOsP_3$	$C_{82}H_{106}Cl_2O_2Os_2P_6$	$C_{25}H_{41}ClO_3OsP_2$	$C_{44}H_{53}Cl_{11}O_3OsPP_3$	$C_{46}H_{62}ClOOsP_3$	$C_{24}H_{41}Cl_5OOsP_2$
M_r	1002.79	1760.79	677.17	1302.92	949.52	774.96
crystal system	triclinic	monoclinic	monoclinic	triclinic	triclinic	hexagonal
space group	$P\bar{1}$	$P2_1/c$	$P2_1/c$	$P\bar{1}$	$P\bar{1}$	$R\bar{3}$
a [Å]	11.368(2)	21.717(4)	14.893(3)	12.471(3)	11.521(2)	40.181(6)
b [Å]	13.056(3)	12.054(2)	10.429(2)	13.785(3)	14.490(3)	40.181(6)
c [Å]	15.300(3)	29.270(6)	17.768(4)	16.508(3)	14.521(3)	11.566(2)
α [°]	88.39(3)	90	90	102.339(3)	64.86(3)	90
β [°]	78.53(3)	95.72(3)	100.93(3)	94.739(3)	80.42(3)	90
γ [°]	72.48(3)	90	90	93.456(3)	82.20(3)	120
ρ_{calcd} [g cm^{-3}]	1.570	1.534	1.660	1.571	1.461	1.432
Z	2	4	4	2	2	18
$\mu(Mo_{K\alpha})$ [mm^{-1}]	3.403	3.572	4.947	2.972	3.161	4.023
crystal size [mm]	0.2×0.05×0.05	0.1×0.1×0.1	0.4×0.4×0.2	0.1×0.1×0.05	0.05×0.05×0.05	0.2×0.2×0.2
total reflns	20168	83308	22814	9370	17449	34733
unique reflns	6499	12515	9809	7888	7043	5428
$R1/wR2$	0.0347/0.0761	0.0499/0.1338	0.0371/0.0928	0.0569/0.1330	0.0394/0.0721	0.0595/0.1634
residual density [e Å^{-3}]	1.208	2.203	2.116	3.014	0.886	2.938

Design. We thank Dr. Leonid Konstantinovsky for his help with the NMR studies. D.M. holds the Israel Matz Professorial Chair of Organic Chemistry.

[1] a) P. Wang, R. Liu, X. Wu, H. Ma, X. Cao, P. Zhou, J. Zhang, X. Weng, X.-L. Zhang, J. Qi, X. Zhou, L. Weng, *J. Am. Chem. Soc.* **2003**, *125*, 1116–1117; b) S. N. Richter, S. Maggi, S. C. Mels, M. Palumbo, M. Freccero, *J. Am. Chem. Soc.* **2004**, *126*, 13973–13979.

[2] a) H. Liu, J. Liu, R. B. van Breemen, G. R. J. Thatcher, J. L. Bolton, *Chem. Res. Toxicol.* **2005**, *18*, 162–173; b) C. Asche, W. Frank, A. Albert, U. Kuckländer, *Bioorg. Med. Chem.* **2005**, *13*, 819–837; c) P. Wang, Y. Song, L. Zhang, H. He, X. Zhou, *Curr. Med. Chem.* **2005**, *12*, 2893–2913.

[3] H.-U. Wagner, R. Gompper, in *The Chemistry of Quinonoid Compounds* (Ed.: S. Patai), Wiley, New York, **1974**, 1145.

[4] a) G. G. Qiao, K. Lenghaus, D. H. Solomon, A. Reisinger, I. Bytheway, C. Wentrup, *J. Org. Chem.* **1998**, *63*, 9806–9811; b) H. Tomioka, *Pure Appl. Chem.* **1997**, *69*, 837–840.

[5] a) B. Rybtchinski, D. Milstein, *Angew. Chem.* **1999**, *111*, 918–932; *Angew. Chem. Int. Ed.* **1999**, *38*, 870–883; b) M. E. van der Boom, D. Milstein, *Chem. Rev.* **2003**, *103*, 1759–1792; c) D. Milstein, *Pure Appl. Chem.* **2003**, *75*, 445–460.

[6] A. Vigalok, D. Milstein, *Acc. Chem. Res.* **2001**, *34*, 798–807.

[7] a) O. Rabin, A. Vigalok, D. Milstein, *J. Am. Chem. Soc.* **1998**, *120*, 7119–7120; b) O. Rabin, A. Vigalok, D. Milstein, *Chem. Eur. J.* **2000**, *6*, 454–462.

[8] a) A. Vigalok, D. Milstein, *J. Am. Chem. Soc.* **1997**, *119*, 7873–7874; b) A. Vigalok, L. J. W. Shimon, D. Milstein, *J. Am. Chem. Soc.* **1998**, *120*, 477–483.

[9] a) A. Vigalok, D. Milstein, *Organometallics* **2000**, *19*, 2341–2345; b) M. E. van der Boom, Y. Ben-David, D. Milstein, *J. Am. Chem. Soc.* **1999**, *121*, 6652–6656; c) A. Vigalok, B. Rybtchinski, L. J. W. Shimon, D. Milstein, *Organometallics* **1999**, *18*, 895–905.

[10] H. Amouri, J. Le Bras, *Acc. Chem. Res.* **2002**, *35*, 501–510.

[11] S. M. Stokes, Jr., F. Ding, P. L. Smith, J. M. Keane, M. E. Kopach, R. Jervis, M. Sabat, W. D. Harman, *Organometallics* **2003**, *22*, 4170–4171.

[12] R. M. Gauvin, H. Rozenberg, L. J. W. Shimon, D. Milstein, *Organometallics* **2001**, *20*, 1719–1724.

[13] a) D. V. Yandulov, J. C. Bollinger, W. E. Streib, K. G. Caulton, *Organometallics* **2001**, *20*, 2040–2046; b) A. Vigalok, H.-B. Kraatz, L. Konstantinovsky, D. Milstein, *Chem. Eur. J.* **1997**, *3*, 253–260.

[14] N. Rahmouni, J. A. Osborn, A. De Cian, J. Fischer, A. Ezzamarty, *Organometallics* **1998**, *17*, 2470–2476.

[15] a) M. Sacco, G. Vasapollo, C. F. Nobile, A. Piergiovanni, *J. Organomet. Chem.* **1988**, *356*, 397–409; b) J. Zhang, G. Leitus, Y. Ben-David, D. Milstein, *J. Am. Chem. Soc.* **2005**, *127*, 10840–10841; c) J. Zhang, G. Leitus, Y. Ben-David, D. Milstein, *Angew. Chem.* **2006**, *118*, 1131–1133; *Angew. Chem. Int. Ed.* **2006**, *45*, 1113–1115.

[16] J. P. Collman, L. S. Hegedus, J. R. Norton, R. G. Finke, in *Principles and Applications of Organotransition Metal Chemistry*, University Science Books, Mill Valley, CA, **1987**.

[17] S. V. Hoskins, C. E. F. Rickard, W. R. Roper, *J. Chem. Soc. Chem. Commun.* **1984**, 1000–1002.

[18] S. H. Liu, S. T. Lo, T. B. Wen, I. D. Williams, Z. Y. Zhou, C. P. Lau, G. Jia, *Inorg. Chim. Acta* **2002**, *334*, 122–130.

[19] a) R. H. Crabtree, *Angew. Chem.* **1993**, *105*, 828–845; *Angew. Chem. Int. Ed. Engl.* **1993**, *32*, 789; b) P. G. Jessop, R. H. Morris, *Coord. Chem. Rev.* **1992**, *121*, 155–284; c) G. S. McGrady, G. Guilera, *Chem. Soc. Rev.* **2003**, *32*, 383–392; d) M. Yousufuddin, T. B. Wen, S. A. Mason, G. J. McIntyre, G. Jia, R. Bau, *Angew. Chem.* **2005**, *117*, 7393–7396; *Angew. Chem. Int. Ed.* **2005**, *44*, 7227–7230.

[20] M. Gandelman, A. Vigalok, L. Konstantinovski, D. Milstein, *J. Am. Chem. Soc.* **2000**, *122*, 9848–9849.

[21] a) A. Vigalok, B. Rybtchinski, Y. Ben David, L. J. W. Shimon, D. Milstein *Organometallics* **1999**, *18*, 895–905; b) A. Vigalok, D. Milstein, *Organometallics* **2000**, *19*, 2341–2345; c) M. Gandelman, L. Konstantinovski, H. Rozenberg, D. Milstein, *Chem. Eur. J.* **2003**, *9*, 2595–2602; d) M. Gandelman, L. J. W. Shimon, D. Milstein, *Chem. Eur. J.* **2003**, *9*, 4295–4300.

[22] N. Ashkenazi, A. Vigalok, S. Parthiban, Y. Ben-David, L. J. W. Shimon, J. M. L. Martin, D. Milstein, *J. Am. Chem. Soc.* **2000**, *122*, 8797–8798.

[23] G. P. Elliot, N. M. McAuley, W. R. Roper, *Inorg. Synth.* **1989**, *26*, 184–189.

[24] L. J. Farrugia, *J. Appl. Crystallogr.* **1997**, *30*, 565.

[25] A. W. van der Made, R. H. van der Made, *J. Org. Chem.* **1993**, *58*, 1262–1263.

[26] "Processing of X-ray Diffraction Data Collected in Oscillation Mode", Z. Otwinowski, W. Minor, *Methods in Enzymology, Vol. 276: Macromolecular Crystallography, part A*, **1997**, pp. 307–326.

[27] G. M. Sheldrick, SHELXS-97 and SHELXL-97, University of Göttingen, Göttingen (Germany), **1997**.

Received: September 27, 2006
Published online: December 15, 2006

